Water-Assisted and Protein-Initiated Ring-Opening Polymerization of Proline *N*-Carboxyanhydride

Yali Hu,[a,b] Zi-You Tian,[a] Wei Xiong, [a] and Hua Lu[a,*]

[a]Beijing National Laboratory for Molecular Sciences, Center for Soft Matter Science and Engineering, Key Laboratory of Polymer Chemistry and Physics of Ministry of Education, College of Chemistry and Molecular Engineering, Peking University, Beijing 100871, People's Republic of China.

[b]Peking-Tsinghua Center for Life Sciences, Academy for Advanced Interdisciplinary Studies, Peking University, Beijing 100871, People's Republic of China.

Corresponding Author: chemhualu@pku.edu.cn (H.L.)

Abstract

The production of poly-$_{L}$-proline (PLP) via the ring-opening polymerization (ROP) of $_{L}$-proline *N*-carboxyanhydride (ProNCA) is challenging due to a combination of factors, including the stringent requirement of moisture-free conditions, slow monomer conversion, poor control of the molar mass, and premature precipitation of the product in the form of polyproline type I helix. Here, we report water-assisted ROP of ProNCA, which affords well-defined PLP in polyproline II helix in 2-5 minutes. Density functional theory reveals an as-yet-unreported role of water in facilitating proton shift that significantly lowered the energy barrier of the chain propagation. Protein-mediated ROP of ProNCA conveniently affords various protein-PLP conjugates via a grafting-from approach. PLP conjugation not only preserves the biological activities of the native proteins, but also enhances the stability of proteins against extreme conditions. This work provides a simple means and new mechanistic insight to solve a longstanding problem in PLP synthesis and will offer valuable guidance for the development of water-resistant ROP of other NCAs. The facile access of PLP can greatly boost the application potentials of PLP-based functional materials.

Introduction

Proline (Pro) is the only proteinogenic amino acid bearing a secondary amine, which results from a circular side chain that loops back and reconnects with the backbone nitrogen. This pyrrolidine ring creates a sterically hindered nitrogen and constrains the conformation of both the Pro and its preceding amino acid residue. Not surprisingly, the Pro-Pro junction is even more restricted, and to its extreme, poly-$_{L}$-proline (PLP) is a well-known rigid “molecular ruler” adopting either the all-*cis* right-handed type I helix (PPI) in common organic solvents or all-*trans* left-handed type II helix (PPII) in aqueous solution, respectively.[1-2] In naturally occurring proteins, proline-rich regions (PRR) in PPII helices play important roles in regulating protein-protein and protein-nucleic acid interactions, signaling, mechanical elasticity, transcription activation, immune response, etc.[3-6] In materials science, there is also a rapidly growing interest in proline or hydroxyproline-derived polymers.[7-9] PLP derivatives have also demonstrate utility as mimics of antifreeze protein,[10] building

blocks for hierarchical self-assembly,[11] templates for controlling nanoparticle growth,[12] gelators,[13] molecular identities controlling distances,[14] antimicrobial[15] and cell-penetrating agents,[16] etc.

Despite the aforementioned progress, research to unlock the full application potential of PPII-helical PLP has been handicapped by the difficulty in synthesizing well-defined, high-molecular-weight (M_n) PLP, presumably due to the high steric hindrance and conformational restriction of Pro. This is evident even in native biosynthesis, where translation of Pro-rich sequences often induces ribosome stalling.[17-18] In chemical synthesis, the construction of a Pro-Pro junction via solid-phase peptide synthesis (SPPS) or native chemical ligation (NCL) is known to be notoriously inefficient and thus impractical for extending an oligoproline array beyond 20 repeating units.[19-20] A number of early literature reports showed the ROP of proline *N*-carboxyanhydride (ProNCA) to be a viable alternative, but the requirement of a strong base such as sodium methoxide inevitably resulted in racemization.[21] An additional caveat is that the M_n of PLP in these studies was estimated solely from viscosity. ROP of ProNCA was achieved in several recent studies using primary or secondary amines in dry pyridine, dioxane, or acetonitrile (ACN) under high vacuum or a continuous nitrogen flow.[13, 22-23] Currently, the best results were reported by Gkikas et al., who attained a M_n up to 13 × 10^3 g/mol and dispersity ($Đ = M_w/M_n$) of 1.23 based on size exclusion chromatographic (SEC) analysis in water/ACN (80/20).[22] Despite the accomplishment, a major flaw of all methods is that PLP would precipitate prematurely in the organic solvent as PPI helix. As a result, it took more than a week to reach 60-80% monomer conversion, and laborious dialysis procedures were later needed to obtain water-soluble, PPII-helical PLP (Scheme 1). Understandably, the tedious and inefficient synthetic method has proved to be a bottleneck for research on the biomedical and materials application of PLP.

Controlled methodologies for the ROP of NCAs have bloomed in the past decade.[24-33] Even more encouragingly, the field is embracing the ROP in open vessels with aqueous solution.[34-37] To name a few, Cheng, Heise, Lecommandoux, and Bonduelle recently demonstrated that the ROP of NCAs r at the water-oil interface, oil-in-water emulsion, or even pure aqueous solutions. These pioneering works opened up a new avenue for developing water-tolerant ROP of NCAs, but were not without limitations. As a start, the reactions were all conducted in a biphasic system, where the actual ROP occurred exclusively in the organic phase under the protection of either PEG or a

surfactant. Furthermore, only hydrophobic polypeptides were produced. It is also worth noting that in some of the above studies 3-24 h were needed to achieve complete monomer conversion. Till now, aqueous-phase ROP of NCAs that generates PLP or other water-soluble polypeptides remains elusive.

Herein, we report the production of well-defined PLP with predictable M_ns up to 18.7 × 10^3 g/mol and $Đ$ in the range of 1.1-1.2, via the unexpected amine-initiated, water-assisted ROP of ProNCA in mixed ACN/H_2O (Scheme 1). In sharp contrast to previous methods, which typically require weeks to obtain PPII-helical PLP, here, complete monomer conversion to product was achieved within a few seconds to less than 5 min without induction. Density functional theory (DFT) calculations of the modal chain propagation reaction revealed that water played an as-yet-unreported role in assisting both the nucleophilic attack and the hydrogen migration, which reduced the overall energy barrier of the polymerization by 7.1 kcal/mol. We also demonstrated that our method could be applied to the synthesis of protein-PLP conjugates via the site-specific grafting-to or randomly-labeled grafting-from approachs. Importantly, the PLP-modification dramatically enhanced the stability of DHFR under extreme conditions while maintaining its enzymatic activity, highlighting the potential of PLP as a fully "natural" and degradable polypeptide for industrial and biomedical applications.

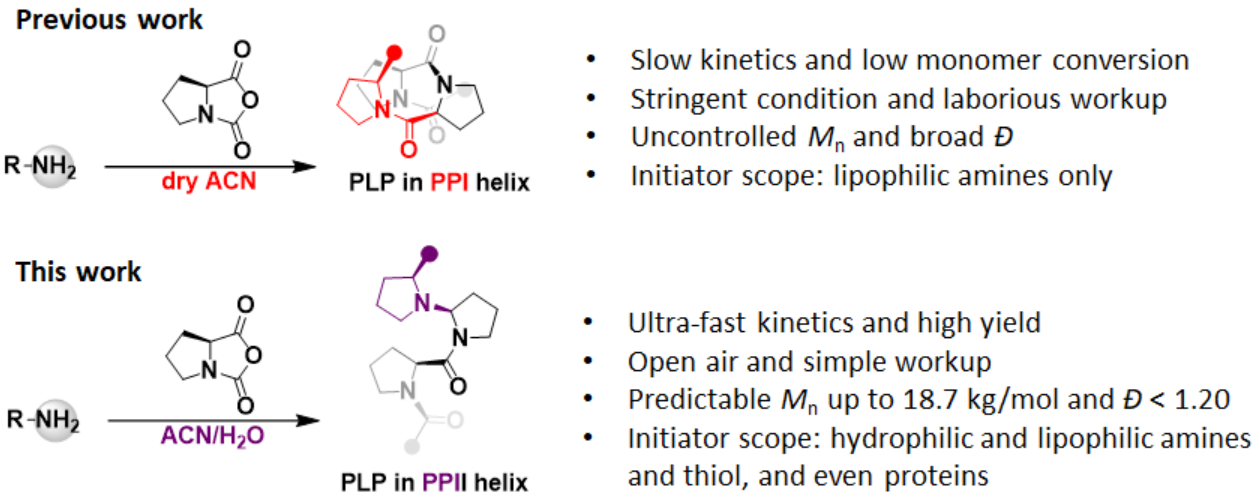

Scheme 1

Results

Highly pure ProNCA was prepared using a moisture-resistant method developed by our lab recently,[38] which significantly simplified the previous laborious workup procedure and offered substantial yield improvement over previous methods from 30% to 72% (see SI). We began our study by first performing primary amine-initiated ROP of ProNCA in dry ACN in a glovebox. Kinetic characterization uncovered an unexpected and unreported two-stage reaction pattern, consisting of an initial stage that lasted roughly 30 min with monomer conversion rapidly reaching ~30%, followed by a second stage in which another 10% of the monomer was slowly consumed over 2 days (Figure 1A-B, blue curves). SEC analysis of the PLPs obtained from different reaction time points consistently showed bimodal peaks with no significant increase in M_n after 30 min of polymerization (Figure 1C, blue curve, and Figure S1). Because the precipitation of PLP occurred quickly after the onset of polymerization (Figure 1D), we hypothesized that this sequestered the growing PLP chain from the organic phase (i.e. ACN), leading to slow, uncontrolled polymerization that was the hallmark of the second stage. We further hypothesized that the above problem could be solved by adding water to the reaction to form a homogenous mixture. We thus tested eight common organic solvents, each mixed with water (v/v =1/1) to serve as the solvent for the ROP of ProNCA. To our great surprise, polymerization in ACN/H_2O was extraordinarily fast and seemed to be well-controlled (Figure 1A-B, red curves), as evidenced by the generation of visible CO_2 bubbles immediately upon addition of initiator (Figure 1E and supplementary video), the consumption of almost all monomer in less than 2 min at 10 ^oC, and a symmetric unimodal SEC trace of the resulting polymer at the end (Figure 1C). Of note, ProNCA dissolved in mixed ACN/H_2O without an initiator retained more than xx% intact at xx min, suggesting the rate of NCA hydrolysis in ACN/H_2O was significantly slower than that of ROP. A slightly slower ROP was observed in THF/H_2O, whereas all other solvent combinations led to bimodal/broader SEC traces (Figure S2).

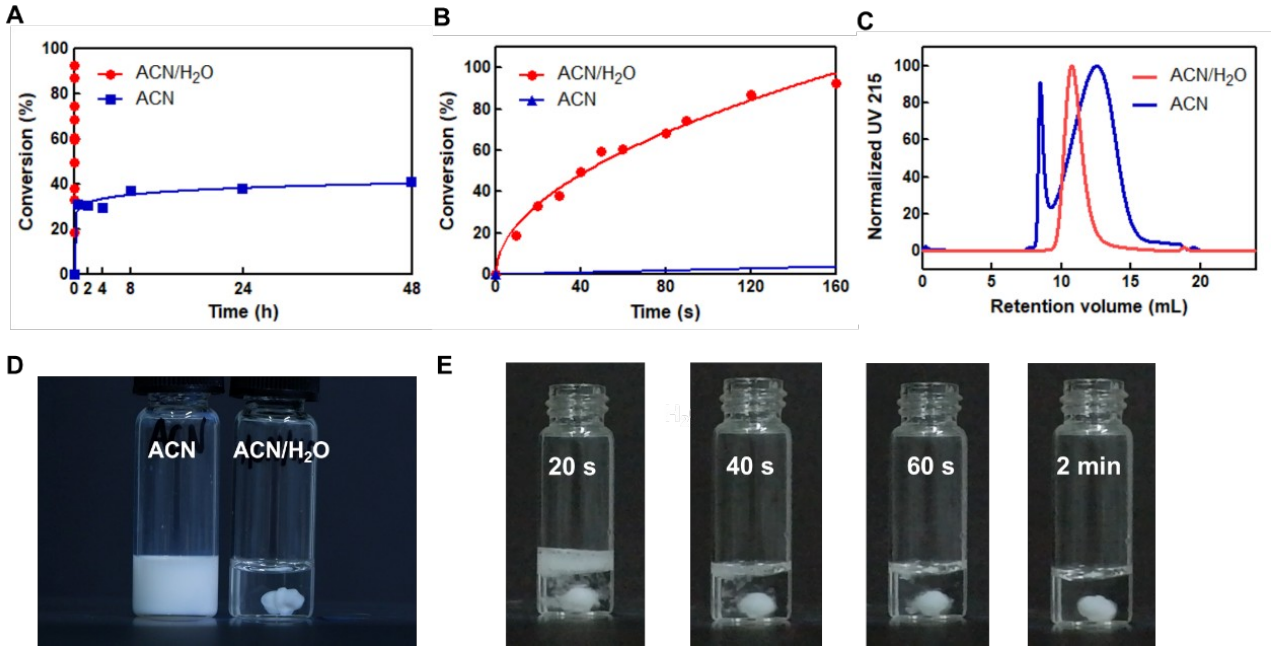

Figure 1. Comparison of the ROP of ProNCA in pure ACN (blue curves) and mixed ACN/H_2O (red curves). (A) Conversions of ProNCA over time and (B) the zoomed in period of the first 160 s. (C) SEC of the PLP produced in CAN and mixed ACN/H_2O. (D) Photographs of the reactions in ACN (left) and mixed ACN/H_2O (right). (E) Snapshots of the ROP of ProNCA in mixed ACN/H_2O showing visible bubbles. $[ProNCA]_0/[I] = 100/1$.

Subsequent reaction optimization in ACN/H_2O yielded the following findings. First, unimodal SEC traces could be obtained at all tested temperatures in the range of 0 to 65 °C, with an inverse correlation between M_n and temperature (Figure S3). Second, pH variation between 5.0 and 9.0 seemed to have negligible effect on the M_n, though the ROP tended to be slightly faster in a more alkaline environment (Figure S4). Third, an initial monomer concentration ($[ProNCA]_0$) above 50 mg/mL was necessary to ensure both fast reaction and good M_n control (Figure S5). Fourth, a H_2O content of 40-60% was optimal; insufficient H_2O would not completely dissolve PLP, whereas too much H_2O appeared to be detrimental to M_n control, likely due to the increased reaction competition from monomer hydrolysis (Figure S6). Fifth, ionic strength (i.e. concentration of NaCl) did not seem to play a significant role in regulating the distribution of M_n (Figure S7).

We next characterized the reaction kinetics, M_n, $Đ$, end group, and chain extension to examine whether the ROP was fully living/controllable (Figure 2). The polymerization was found to follow

first-order kinetics (Figure 2A-B and S8-10) versus monomer concentration at various molar ratios of monomer to initiator ($[ProNCA]_0/[I]$). The apparent chain propagation rate constant (k_{app}) was calculated from the slope of each linear line and shown to range from 0.0065 to 0.053 s^{-1}. Thus, the real chain propagation rate constant (k_p) was estimated to be 1.95-4.00 M^{-1} s^{-1}, which is ~2 to 3 magnitude fold faster than normal amine-initiated ROP of NCAs in organic solvents. Varying the feeding $[ProNCA]_0/[I]$ ratio led to a linear increase in the M_n of the PLP products, which were all within 5% deviation from the theoretical values (Figure 2C and Table 1, entry 2-5). PLPs of various M_n all displayed unimodal SEC peaks, with $Đ$s in the range of 1.1-1.2 (Figure 2C inset and Table 1, entry 2-5). The highest M_n was obtained at a $[ProNCA]_0/[I]$ ratio of 200/1, yielding PLP of 18.7 × 10^3 g/mol (Table 1, entry 5). It should be pointed out that the SEC traces showed tailing at the $[ProNCA]_0/[I]$ ratio of 200/1, a limitation of the method. This is likely the result of a small portion of monomer hydrolyzed at the late stage of the polymerization, which initiated the ROP and gave PLP with smaller M_n. The linear correlation between M_n and the degree of monomer conversion implied that the polymerization proceeded via a chain-growth mechanism (Figure 2D). The livingness of the ROP was further confirmed by the facile chain extension from an in situ-generated PLP macroinitiator (Figure 2E). Matrix-assisted laser desorption/ionization-time of flight (MALDI-TOF) mass spectrometric analysis of the PLP product from benzyl amine-mediated ROP at a $[ProNCA]_0/[I]$ ratio of 20/1 suggested a well-defined end group fidelity, with all peaks in the mass spectrum assignable to the molecular formula of $BnNH–Pro_n–H$ (with the addition of H^+, Na^+, or K^+) (Figure 2F). Compared to the conventional method that requires time-consuming dialysis to induce an incomplete PPI-to-PPII transition of the PLP product (Table 1, entry 1), ROP in mixed ACN/H_2O allowed the direct acquisition of water-soluble PLP at 83-92% purification yield. This high separation yield once again confirmed the high monomer conversion. Circular dichroism (CD) spectroscopy confirmed that the PLP prepared in mixed ACN/H_2O existed as left-handed PPII helix (Figure 2G), whereas the ROP of $_D$-ProNCA and $_{DL}$-ProNCA furnished right-handed PPII-helical and disordered PDP and PDLP products, respectively (Figure 2G). Together, the above results unambiguously proved that the ROP of ProNCA in mixed ACN/H_2O was robust under various conditions and afforded PLPs with highly controlled structural characters.

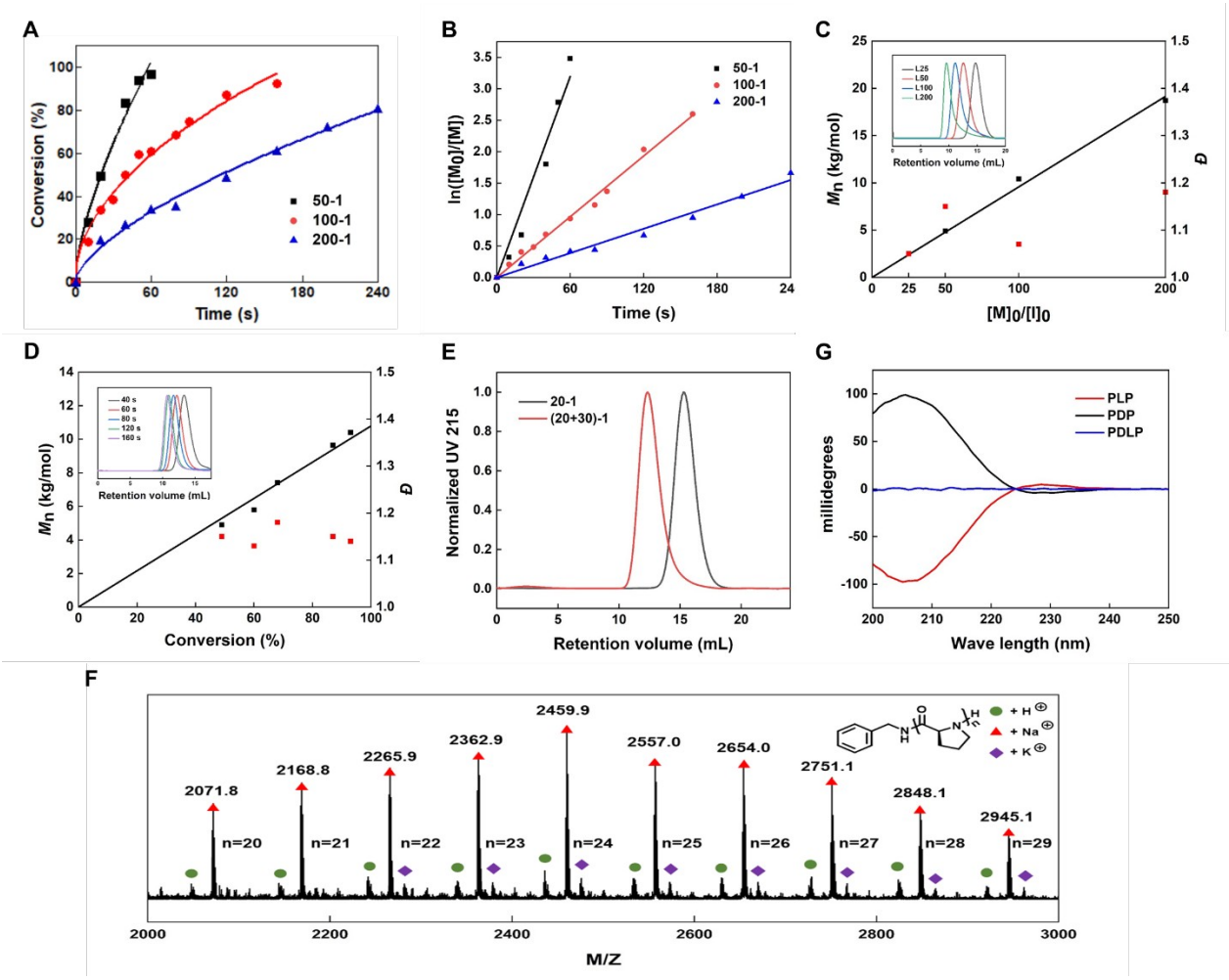

Figure 2. Benzyl amine-initiated controlled ROP of ProNCA in mixed ACN/H_2O. (A) Conversions of ProNCA over time and (B) plots of first-order kinetics of the ROP at different $[M]_0/[I]_0$ ratios. (C-D) Plots of M_n and $Đ$ of PLP (C) as a function of $[M]_0/[I]_0$ ratio and (D) conversion of ProNCA ($[M]_0/[I]_0$ = 100/1). (E) SEC trances showing the chain extension of PLP from a 20-mer to a 50-mer. (F) MALDI-TOF mass spectrum of PLP 25-mer. (G) CD spectra of PLP, PDP, and PDLP showing typical left-handed and right-handed PPII helix, and no secondary conformation, respectively.

Table 1. Ultra-fast ROP of ProNCAs in mixed ACN/H_2O

Entry	solvent	$[ProNCA]_0/[I]$	Time	M_n^{cal} (kg/mol)[a]	M_n^{obt} (kg/mol)[b]	$Đ$[b]	Yield (%)[c]	$[\Theta]_{229}$ (deg cm^2 $dmol^{-1}$)
1	ACN	100	2 days	9.8	/[d]	/[d]	48	1381
2	ACN/H_2O	25	< 1 min	2.5	2.5	1.05	85	2081
3	ACN/H_2O	50	< 2 min	5.0	5.0	1.15	89	2126
4	ACN/H_2O	100	< 3 min	9.8	10.3	1.07	88	2226
5	ACN/H_2O	200	< 5 min	19.5	18.7	1.18	92	2393
6	ACN/H_2O	50[e]	< 2 min	5.0	5.1	1.10	83	-2354
7	ACN/H_2O	50[e]	< 2 min	5.0	4.6	1.12	87	32

[a]calculated from feeding $[ProNCA]_0/[I]_0$; [b]obtained from aqueous SEC equipped with a multi-angle light scattering detector in 1×PBS (pH = 7.4) mobile phase; d*n*/d*c* (658 nm) values were measured as 0.178 for PLP and 0.175 for PDLP. [c]purification yield after PD-10 column. [d]SEC gave bimodal peaks as shown in Figure 1C. [e]$_{D-}$ and $_{DL-}$ ProNCA were used as monomer in entry 6 and 7, respectively.

The enhanced solubility of PLP in water was certainly a contributing factor for accelerating the ROP of ProNCA in ACN/H_2O. However, a significant rate enhancement was also observed in 80%/20% ACN/H_2O during our condition optimization (Figure S6), at which the PLP was still insoluble. Even more interestingly, the ROP could be accelerated even when a catalytic amount of H_2O was added to ACN. Collectively, the unusually rapid polymerization in mixed ACN/H_2O over normal ROP of NCAs in organic solvent indicated that, there must be other contributing factors of water apart from solubilization, solvent polarity, or dielectric constant. We first ruled out the possibility of ProNCA hydrolysis as the monomer remained intact for 4 min under the ROP condition without an amine initiator, which was longer than the time required for complete ROP. We next disapproved the existence of cooperative polymerization, a self-accelerating mechanism that was elegantly demonstrated by Cheng and coworkers in the ROP of NCAs that producing α-helical polypeptides. Presumably, we did not observe the existence of an induction period that corresponded to the nucleation stage, a well-known kinetic feature of cooperative polymerization, in any of our kinetic studies (Figure 2A-B). Moreover, we observed no significant difference in the polymerization rate or M_n control between the ROP of $_{L-}$, $_{D-}$, and $_{DL}$-ProNCA, regardless of whether the reaction was initiated by benzyl amine (Table 1, entry 3, 6, and 7) or the macroinitiator PLP

(Figure S11).

We then evaluated another plausible hypothesis that proposes a role of water molecules in assisting the rate-determining step (RDS). We conducted detailed DFT study of a model chain-propagation reaction (Figure 3) using (*S*)-*N*, *N*-dimethylpyrrolidine-2-carboxamide (SM) to represent the reactive chain end. It was found that the reaction in pure ACN showed a three-stage propagation process that consisted of nucleophilic addition, intramolecular proton shift, and decarboxylation. The transition state **TS2a** showed the highest activation Gibbs free energy at 26.6 kcal/mol, leading to the surprising finding that the proton shift, rather than the nucleophilic attack, was the RDS in the ROP of ProNCA in pure ACN (Figure 3 and Figure S12-13). Of note, the proton shift required the newly formed amide bond in **TS2a** to assume a *cis* conformation, which offered a potential explanation of why polymerization in ACN afforded PPI-helical PLP. In the presence of H_2O, however, the same model reaction above was found to follow an alternative mechanistic route that could be roughly divided into stages of nucleophilic addition, ring-opening, intramolecular proton shift, and decarboxylation. A key deviation from the ROP in anhydrous ACN was that H_2O, as both a hydrogen bonding donor and acceptor, helped arrange SM and ProNCA in proximity to each other, which facilitated nucleophilic addition (Figure 3 and S14-15, **TS1c)**. The activation Gibbs free energy of **TS1c** was 19.5 kcal/mol, which was shown to be the highest energy barrier for the whole process. In the proton shift stage, hydrogen bonding to water molecules stabilized the amide bond of the zwitterionic intermediate **Int4c** in a *trans* conformation, and facilitated the subsequent proton shift, leading to the final, spontaneous decarboxylation of **Int5c**. Overall, the presence of H_2O shifted the RDS to the nucleophilic addition step and dramatically lowered the overall energy barrier of the chain propagation by 7.1 kcal/mol, which could accelerate the ROP rate up to 5 order of magnitude (Figure 3 and SI). The DFT results thus provided a plausible explanation of why water-assisted ROP of ProNCA was fast and furnished PPII-helical products.

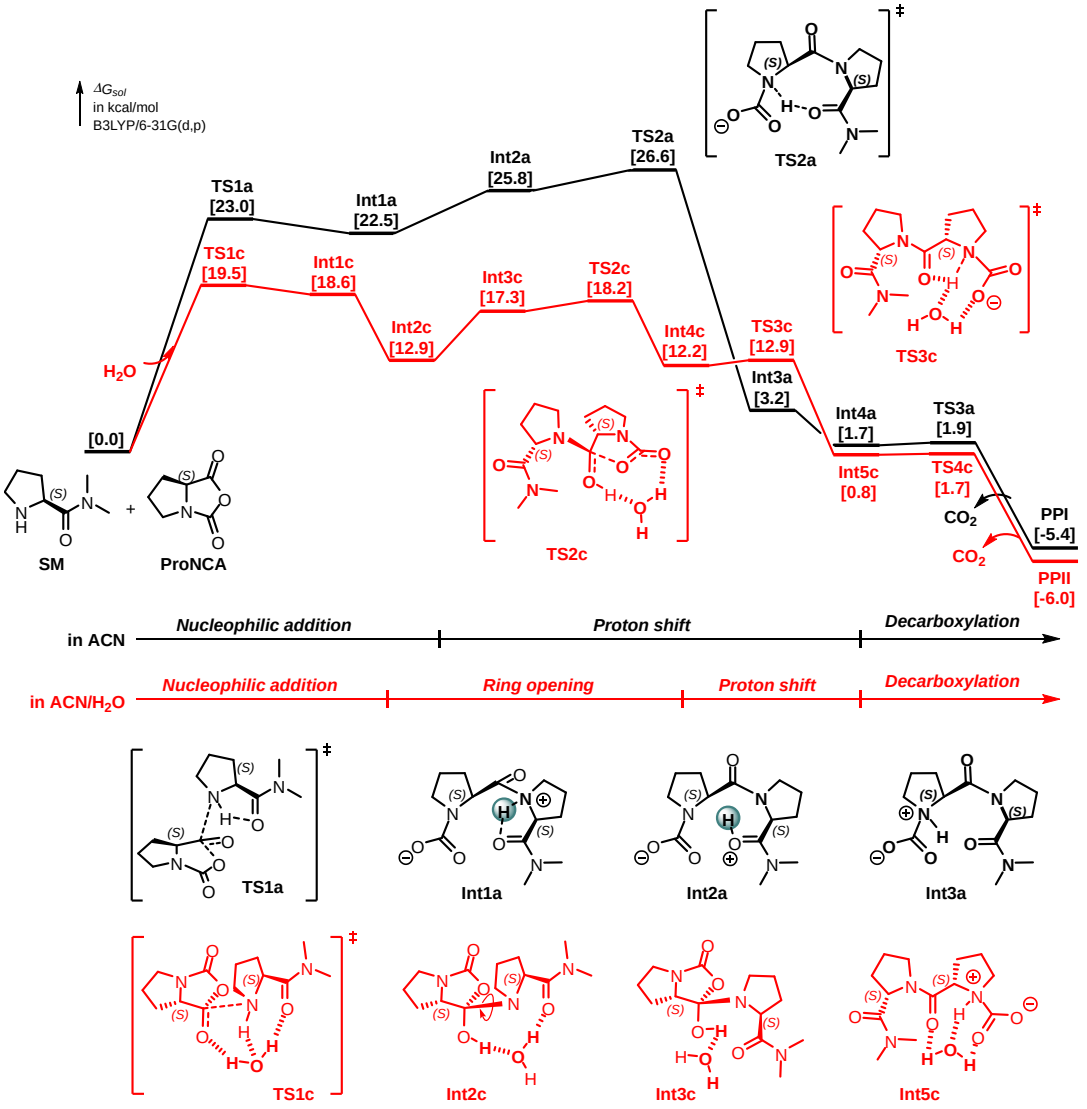

Figure 3. DFT calculations of model chain propagation reactions reveal plausible pathways for the ROP of ProNCA in dry ACN (black) and mixed ACN/H_2O (red).

One limit of previous methods is the scope of initiators was restricted to hydrophobic amines only due to the use of pure organic solvents. This limitation could be easily overcame in our system. To assess the scope of initiators, we screened a variety of secondary alkyl and aryl amines, alkyl and phenyl mercaptanes, as well as complex biomolecules such as ε-amine of lysine and glucosamine (Figure 4A). The resulting PLP produced in ACN/H_2O all showed unimodal and narrow SEC peaks, indicating excellent control of M_n (Figure 4B, and Figure S16-22). Remarkably,

both ^{1}H NMR and MALDI-TOF analyses demonstrated that PLP bearing exclusively *p*-methyl phenyl thioester (MPT) at the *C*-terminus could be generated by using *p*-methyl phenyl mercaptane as initiator (Figure 4C and S22). This in situ-generated functional group would be particularly useful for the facile bioconjugation of PLP via NCL.[8, 39] Indeed, reaction of a MPT-functionalized PLP (MPT-PLP, M_n = 4.9 kg/mol, $Đ$ = 1.15) with enhanced green fluorescent protein (EGFP) bearing an *N*-cysteine (Cys-EGFP) under biological relevant conditions yielded the *N*-terminal specific PLP-EGFP conjugate in 73% yield (Figure 4D-E).

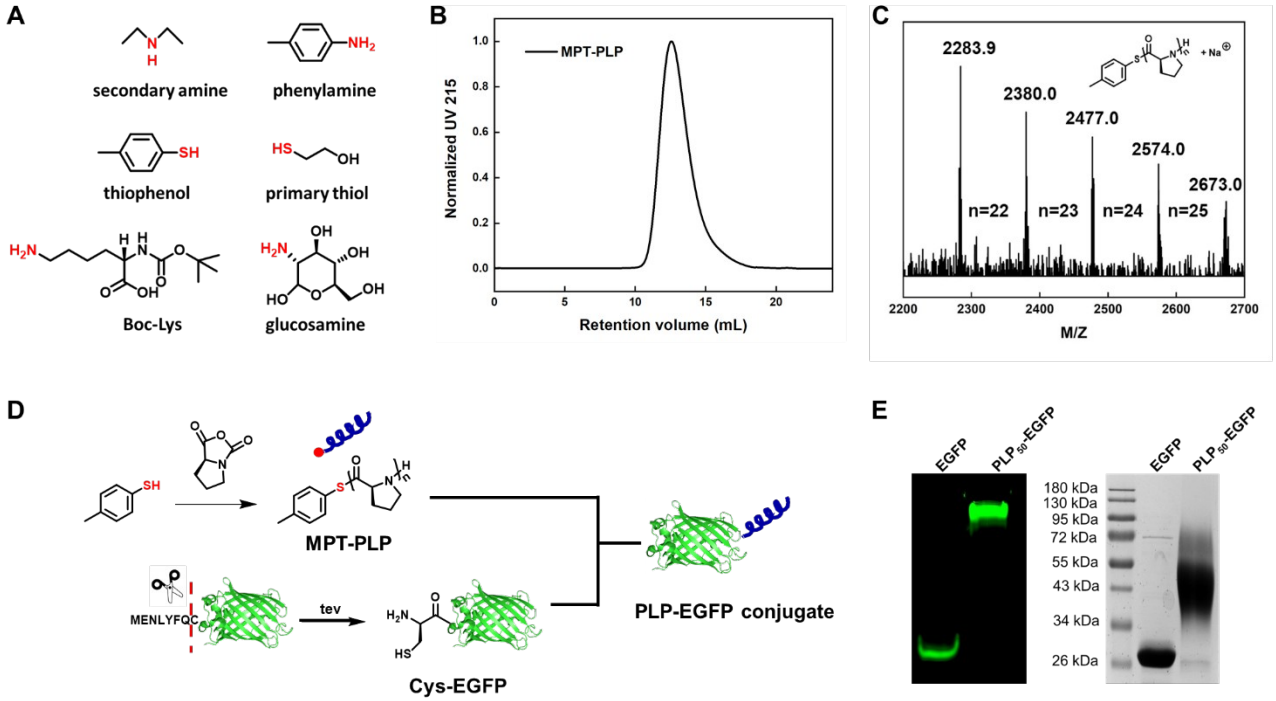

Figure 4. (A) Scope of small molecular initiators for the ROP of ProNCA in mixed ACN/H_2O. (B) The SEC trace and (C) MALDI-TOF spectrum of MPT-PLP. (D) Scheme of PLP-EGFP synthesis via the site-specific NCL of MPT-PLP and Cys-EGFP. (E) Native (left) and SDS-PAGE (right) analysis of the purified PLP-EGFP conjugate.

Encouraged by the robustness of the ROP at various pH and salt concentrations (Figure S4&7), we further examined whether amine-bearing proteins could be utilized as macroinitiator to generate protein-PLP conjugates *in situ* (Figure 5A).[40-47] The protein-initiated ROP of various NCAs, including ProNCA, was previously tested in 1950-1960s but later discontinued.[48-49] Here, we decided to revisit this topic using the fast ROP in mixed ACN/H_2O. Gratifyingly, 10-min ROP of

ProNCA at 10 °C in ACN/PBS (*v*/*v* = 1/1, pH 7.4) in EGFP solution led to the efficient formation of EGFP-PLP conjugates based on SDS-PAGE analysis. When the feeding concentration of ProNCA was increased from 1.0 to 50 mg/mL, the products, appearing as smear bands, gradually shifted to higher molecular weight regions, with the upper limit exceeding 180 kDa (Figure 5B). The average molecular weight of the EGFP-PLP conjugates was close to the theoretically predicted value, and no free EGFP was observed in the crude reaction mixture. These results all indicated quantitative initiation efficiency and controlled PLP growth. Of note, the fluorescence of EGFP was well-maintained throughout the ROP and purification processes (Figure 5B inset). The ROP of PLP using dihydrofolate reductase (DHFR) as initiator yield a product profile with a similar molecular weight distribution (Figure 5C). Moreover, the resulting three DHFR-PLP conjugates exhibited almost identical enzymatic activity as untreated wt-DHFR (Figure S23). Remarkably, one DHFR-PLP conjugate was found to retain ~ 80% or 96% of the enzymatic activity of the native protein after 12 h of ethanol treatment or 10 min of heat shock at 80 °C, respectively; in contrast, wt-DHFR retained only 20% and 65% of the catalytic activity after the same ethanol or heat treatment, respectively (Figure 5D).

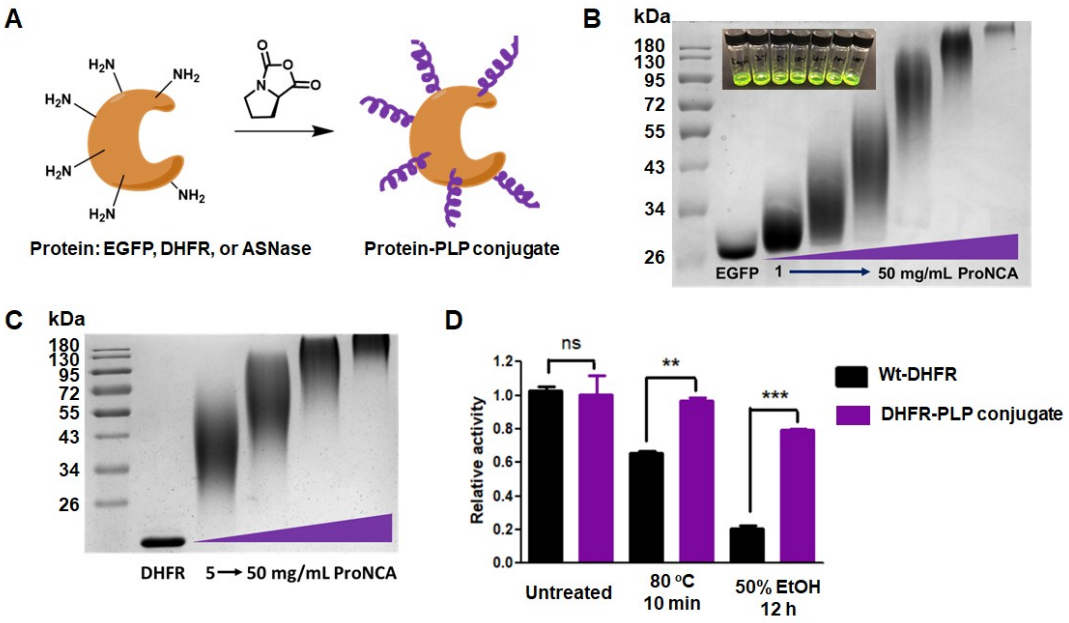

Figure 5. Protein-initiated ROP of ProNCA and applications of the Protein-PLP conjugates. (A) Cartoon illustration of the protein-initiated ROP of ProNCA. (B) SDS-PAGE characterization; inset: snapshots of the EGFP-PLP conjugates. (C) SDS-PAGE characterization of the DHFR-PLP conjugates. (D) DHFR enzymatic assay under normal or extreme conditions for wt-DHFR (black

bars) and the DHFR-PLP conjugate (purple bars). P value was determined by ANOVA (ns = no significant difference; * P < 0.05; ** P < 0.01; *** P < 0.001).

Discussion and Conclusions

PPII helices are among the most prevalent structural motifs in proteins, and PRRs are frequently involved in essential cellular processes such as cell signaling and binding. Synthetic PPII-helical PLP can emulate the unique structural and functional roles of PPII helices and PRR, ultimately leading to the creation of novel materials for numerous biological and biomedical applications. However, conventional methods for PLP synthesis were slow and inefficient, required harsh, moisture-free conditions, allow little control of M_n and $Đ$, and resulted in the premature precipitation of the product as PPI helix. In the current study, we demonstrated that the reaction time for the ROP of ProNCA could be dramatically shortened from weeks to less than 5 minutes by simply adding water as a co-solvent (Figure 1). Comprehensive kinetic studies and characterizations of the resultant PLP products confirmed the highly controlled/living nature of the ROP (Figure 3 and Table 1). While moisture-tolerant ROP of NCAs has gained considerable attraction in recent years, the polymerization reaction is still confined to the organic phase and/or the biphasic interface. Here, we achieved ROP of NCA in homogeneous systems with water as a major co-solvent and an unexpected aid rather than a detriment. Key contributing factors to the excellent reaction control of the ROP in water included enhanced solubility of PLP and the unexpected water-assisted acceleration of the polymerization process, which allowed it to kinetically outcompete monomer hydrolysis. Most importantly, our DFT results revealed the crucial mechanistic role of water molecules in facilitating a hydrogen shift that substantially lowered the energy barrier of the chain propagation by ~ 7.1 kcal/mol (Figure 3). Robust polymerization control was attainable under a broad range of biological relevant conditions using various initiators, which, together with the fast kinetics, enabled the facile synthesis of well-defined protein-PLP conjugates via both grafting-to (N-terminal specific) and grafting-from (lysine specific) approaches (Figure 4 and 5). The in-situ growth of PLP from the surfaces of native proteins was intrinsically more efficient than the grafting-to approach, and the purification is much simpler.

The function of PLP is yet to be fully exploited. Here, even though the grafting-from generated

conjugates were labeled in a non-specific fashion with the use of an organic solvent, some of the PLP-grafted proteins retained their biological functions with minimal compromise, as demonstrated by the full preservation of the EGFP fluorescence and DHFR catalytic activity. There are three plausible reasons for this result. First, the ultra-fast kinetics of ROP allowed product generation within 10 min, and thus minimized the detrimental effect posed by exposure to the organic solvent. Second, it appeared that the growth of PLP on the surface of DHFR enhanced the resistance to organic solvent exposure dramatically (Figure 5D). Third, the substrates of the DHFR-catalyzed reaction were small molecules, whose diffusion and binding to the catalytic pocket was generally insensitive to the steric hindrance of PLP. Although this grafting-from approach might not be extremely suitable for proteins whose biological functions were dependent on one or more accessible lysines, it could still find broad applications using a variety of peptides, hormones, reporter proteins, and enzymes that were lysine-independent. Our group is testing the use of PLP modification as a potential replacement to PEGylation using a first-line anticancer therapeutic protein ASNase as model, which has showed encouraging in vivo improvements and will be reported separately soon. These results indicated that PLP, being biodegradable and completely natural, holds great potential as an outstanding alternative to the nondegradable PEG, whose clinical limitations are increasingly recognized in recent years.[50-55]

Overall, this work provided a simple means and new mechanistic insight to solve a longstanding problem in PLP synthesis and would offer valuable guidance for the development of water-resistant ROP of other NCAs. The facile access of PLP could facilitate understanding of the biophysical and biological roles of PRRs in natural proteins and greatly boost the application potentials of PLP-based functional materials.

Acknowledgements

This work is supported by the National Key Research and Development Program of China (2019YFA0904203) and the National Natural Science Foundation of China (21722401). Z.Y.T. thanks the National Postdoctoral Program for Innovative Talents (BX20190004). The computation was supported by High-performance Computing Platform of Peking University. W.X. thanks the

fellowship of China Postdoctoral Science Foundation (2020M680193). The authors acknowledge Hao Wang, Ruichi Zhao, and Yiming Sun for their helps on providing some of the raw materials used in this work. The authors thank National Center for Protein Sciences at Peking University for assistance with FPLC-MALS.

Author Contributions

Y.L.H. and H.L. conceived the idea, designed the experiments, analyzed the data, and wrote the manuscript. Y.L.H. conducted most experiments; Z.Y.T. performed the DFT calculation; W.X. performed all of the MALDI-TOF analysis. All of the authors read and approved the final version of manuscript.

Additional Information

Supporting information: experimental protocol, condition screening, supplementary figures (SEC, ^{1}H NMR, MALDI-TOF mass spectra…etc); DFT coordination parameters.

Competing Interests

The authors declare no competing interests.

References

1. Best, R. B.; Merchant, K. A.; Gopich, I. V.; Schuler, B.; Bax, A.; Eaton, W. A., Effect of flexibility and cis residues in single-molecule FRET studies of polyproline. *Proc. Natl. Acad. Sci. U. S. A.* **2007,** *104* (48), 18964-18969.
2. Schuler, B.; Lipman, E. A.; Steinbach, P. J.; Kumke, M.; Eaton, W. A., Polyproline and the "spectroscopic ruler" revisited with single-molecule fluorescence. *Proc. Natl. Acad. Sci. U. S. A.* **2005,** *102* (8), 2754-2759.
3. Kay, B. K.; Williamson, M. P.; Sudol, P., The importance of being proline: the interaction of proline-rich motifs in signaling proteins with their cognate domains. *FASEB J.* **2000,** *14* (2), 231-241.
4. Mahoney, N. M.; Janmey, P. A.; Almo, S. C., Structure of the profilin-poly-L-proline complex involved in morphogenesis and cytoskeletal regulation. *Nat. Struct. Biol.* **1997,** *4* (11), 953-960.
5. Yu, H. T.; Chen, J. K.; Feng, S. B.; Dalgarno, D. C.; Brauer, A. W.; Schreiber, S. L., Structural Basis for the Binding of Proline-Rich Peptides to Sh3 Domains. *Cell* **1994,** *76* (5), 933-945.
6. Ruggiero, M. T.; Sibik, J.; Orlando, R.; Zeitler, J. A.; Korter, T. M., Measuring the Elasticity of Poly-L-Proline Helices with Terahertz Spectroscopy. *Angew. Chem., Int. Ed.* **2016,** *55* (24), 6877-

6881.
7. Tian, Z.-Y.; Wang, S.; Lu, H., Hydroxyproline-derived biomimetic and biodegradable polymers. *Curr. Opin. Solid State Mater. Sci.* **2021,** *25* (2), 100902.
8. Yuan, J.; Shi, D.; Zhang, Y.; Lu, J.; Wang, L.; Chen, E.-Q.; Lu, H., 4-Hydroxy-l-Proline as a General Platform for Stereoregular Aliphatic Polyesters: Controlled Ring-Opening Polymerization, Facile Functionalization, and Site-Specific Bioconjugation. *CCS Chem.* **2020,** *2* (5), 236–244.
9. Yuan, J.; Xiong, W.; Zhou, X.; Zhang, Y.; Shi, D.; Li, Z.; Lu, H., 4-Hydroxyproline-Derived Sustainable Polythioesters: Controlled Ring-Opening Polymerization, Complete Recyclability, and Facile Functionalization. *J. Am. Chem. Soc.* **2019,** *141* (12), 4928-4935.
10. Graham, B.; Bailey, T. L.; Healey, J. R. J.; Marcellini, M.; Deville, S.; Gibson, M. I., Polyproline as a Minimal Antifreeze Protein Mimic That Enhances the Cryopreservation of Cell Monolayers. *Angew. Chem., Int. Ed.* **2017,** *56* (50), 15941-15944.
11. Gkikas, M.; Haataja, J. S.; Seitsonen, J.; Ruokolainen, J.; Ikkala, O.; Iatrou, H.; Houbenov, N., Extended Self-Assembled Long Periodicity and Zig-Zag Domains from Helix-Helix Diblock Copolymer Poly(gamma-benzyl-L-glutamate)-block-poly(O-benzyk-hydroxyproline). *Biomacromolecules* **2014,** *15* (11), 3923-3930.
12. Upert, G.; Bouillere, F.; Wennemers, H., Oligoprolines as Scaffolds for the Formation of Silver Nanoparticles in Defined Sizes: Correlating Molecular and Nanoscopic Dimensions. *Angew. Chem., Int. Ed.* **2012,** *51* (17), 4231-4234.
13. Gkikas, M.; Avery, R. K.; Olsen, B. D., Thermoresponsive and Mechanical Properties of Poly(L-proline) Gels. *Biomacromolecules* **2016,** *17* (2), 399-406.
14. Dobitz, S.; Aronoff, M. R.; Wennemers, H., Oligoprolines as Molecular Entities for Controlling Distance in Biological and Material Sciences. *Acc. Chem. Res.* **2017,** *50* (10), 2420-2428.
15. Kuriakose, J.; Hernandez-Gordillo, V.; Nepal, M.; Brezden, A.; Pozzi, V.; Seleem, M. N.; Chmielewski, J., Targeting Intracellular Pathogenic Bacteria with Unnatural Proline-Rich Peptides: Coupling Antibacterial Activity with Macrophage Penetration. *Angew. Chem., Int. Ed.* **2013,** *52* (37), 9664-9667.
16. Fillon, Y. A.; Anderson, J. P.; Chmielewski, J., Cell penetrating agents based on a polyproline helix scaffold. *J. Am. Chem. Soc.* **2005,** *127* (33), 11798-11803.
17. Tanner, D. R.; Cariello, D. A.; Woolstenhulme, C. J.; Broadbent, M. A.; Buskirk, A. R., Genetic Identification of Nascent Peptides That Induce Ribosome Stalling. *J. Biol. Chem.* **2009,** *284* (50), 34809-34818.
18. Pavlov, M. Y.; Watts, R. E.; Tan, Z.; Cornish, V. W.; Ehrenberg, M.; Forster, A. C., Slow peptide bond formation by proline and other N-alkylamino acids in translation. *Proc. Natl. Acad. Sci. U. S. A.* **2009,** *106* (1), 50-54.
19. Sayers, J.; Karpati, P. M. T.; Mitchell, N. J.; Goldys, A. M.; Kwong, S. M.; Firth, N.; Chan, B.; Payne, R. J., Construction of Challenging Proline-Proline Junctions via Diselenide-Selenoester Ligation Chemistry. *J. Am. Chem. Soc.* **2018,** *140* (41), 13327-13334.
20. Townsend, S. D.; Tan, Z. P.; Dong, S. W.; Shang, S. Y.; Brailsford, J. A.; Danishefsky, S. J., Advances in Proline Ligation. *J. Am. Chem. Soc.* **2012,** *134* (8), 3912-3916.
21. Fasman, G. D.; Blout, E. R., High Molecular Weight Poly-L-Proline: Synthesis and Physical-Chemical Studies. *Biopolymers* **1963,** *1* (1), 3-14.
22. Gkikas, M.; Iatrou, H.; Thomaidis, N. S.; Alexandridis, P.; Hadjichristidis, N., Well-Defined

Homopolypeptides, Copolypeptides, and Hybrids of Poly(L-proline). *Biomacromolecules* **2011,** *12* (6), 2396-2406.
23. Muller, D.; Stulz, J.; Kricheldorf, H. R., Secondary Structure of Peptides 14. FT-IR and 13C NMR CP/MAS Investigation of the Helix Stability of Solid Poly(L-Proline)s. *Makromol. Chem. Macromol. Chem. Phys.* **1984,** *185* (8), 1739-1749.
24. Zhao, W.; Lv, Y.; Li, J.; Feng, Z.; Ni, Y.; Hadjichristidis, N., Fast and selective organocatalytic ring-opening polymerization by fluorinated alcohol without a cocatalyst. *Nat. Commun.* **2019,** *10* (1), 3590.
25. Deming, T. J., Facile synthesis of block copolypeptides of defined architecture. *Nature* **1997,** *390* (6658), 386-389.
26. Yuan, J.; Sun, Y.; Wang, J.; Lu, H., Phenyl Trimethylsilyl Sulfide-Mediated Controlled Ring-Opening Polymerization of alpha-Amino Acid N-Carboxyanhydrides. *Biomacromolecules* **2016,** *17* (3), 891-896.
27. Lu, H.; Cheng, J. J., Hexamethyldisilazane-mediated controlled polymerization of alpha-Amino acid N-carboxyanhydrides. *J. Am. Chem. Soc.* **2007,** *129* (46), 14114-14115.
28. Vacogne, C. D.; Schlaad, H., Primary ammonium/tertiary amine-mediated controlled ring opening polymerisation of amino acid N-carboxyanhydrides. *Chem. Commum.* **2015,** *51* (86), 15645-15648.
29. Conejos-Sanchez, I.; Duro-Castano, A.; Birke, A.; Barz, M.; Vicent, M. J., A controlled and versatile NCA polymerization method for the synthesis of polypeptides. *Polym. Chem.* **2013,** *4* (11), 3182-3186.
30. Rasines Mazo, A.; Allison-Logan, S.; Karimi, F.; Chan, N. J.; Qiu, W.; Duan, W.; O'Brien-Simpson, N. M.; Qiao, G. G., Ring opening polymerization of alpha-amino acids: advances in synthesis, architecture and applications of polypeptides and their hybrids. *Chem. Soc. Rev.* **2020,** *49* (14), 4737-4834.
31. Liu, Y.; Li, D.; Ding, J.; Chen, X., Controlled synthesis of polypeptides. *Chin. Chem. Lett.* **2020,** *31* (12), 3001-3014.
32. Tao, X. F.; Li, M. H.; Ling, J., alpha-Amino acid N-thiocarboxyanhydrides: A novel synthetic approach toward poly(alpha-amino acid)s. *Eur. Polym. J.* **2018,** *109*, 26-42.
33. Deming, T. J., Synthesis of Side-Chain Modified Polypeptides. *Chem. Rev.* **2016,** *116* (3), 786-808.
34. Wu, Y.; Zhang, D.; Ma, P.; Zhou, R.; Hua, L.; Liu, R., Lithium hexamethyldisilazide initiated superfast ring opening polymerization of alpha-amino acid N-carboxyanhydrides. *Nat. Commun.* **2018,** *9* (1), 5297.
35. Song, Z.; Fu, H.; Wang, J.; Hui, J.; Xue, T.; Pacheco, L. A.; Yan, H.; Baumgartner, R.; Wang, Z.; Xia, Y.; Wang, X.; Yin, L.; Chen, C.; Rodriguez-Lopez, J.; Ferguson, A. L.; Lin, Y.; Cheng, J., Synthesis of polypeptides via bioinspired polymerization of in situ purified N-carboxyanhydrides. *Proc. Natl. Acad. Sci. U. S. A.* **2019,** *116* (22), 10658-10663.
36. Jacobs, J.; Pavlović, D.; Prydderch, H.; Moradi, M.-A.; Ibarboure, E.; Heuts, J. P. A.; Lecommandoux, S.; Heise, A., Polypeptide Nanoparticles Obtained from Emulsion Polymerization of Amino Acid N-Carboxyanhydrides. *J. Am. Chem. Soc.* **2019,** *141* (32), 12522-12526.
37. Grazon, C.; Salas-Ambrosio, P.; Ibarboure, E.; Buol, A.; Garanger, E.; Grinstaff, M. W.; Lecommandoux, S.; Bonduelle, C., Aqueous Ring-Opening Polymerization-Induced Self-

Assembly (ROPISA) of N-Carboxyanhydrides. *Angew. Chem., Int. Ed.* **2020,** *59* (2), 622-626.
38. Tian, Z.-Y.; Lu, H., *A Robust, Open-Flask, Moisture-Tolerant, and Scalable Route to Unprotected α/β-Amino Acid N-Carboxyanhydrides*. 2020.
39. Hou, Y.; Yuan, J.; Zhou, Y.; Yu, J.; Lu, H., A Concise Approach to Site-Specific Topological Protein-Poly(Amino Acid) Conjugates Enabled by In-situ Generated Functionalities. *J. Am. Chem. Soc.* **2016,** *138* (34), 10995-11000.
40. De, P.; Li, M.; Gondi, S. R.; Sumerlin, B. S., Temperature-regulated activity of responsive polymer-protein conjugates prepared by grafting-from via RAFT polymerization. *J. Am. Chem. Soc.* **2008,** *130* (34), 11288-11289.
41. Bontempo, D.; Maynard, H. D., Streptavidin as a macroinitiator for polymerization: In situ protein-polymer conjugate formation. *J. Am. Chem. Soc.* **2005,** *127* (18), 6508-6509.
42. Boyer, C.; Bulmus, V.; Liu, J. Q.; Davis, T. P.; Stenzel, M. H.; Barner-Kowollik, C., Well-defined protein-polymer conjugates via in situ RAFT polymerization. *J. Am. Chem. Soc.* **2007,** *129* (22), 7145-7154.
43. Russell, A. J.; Baker, S. L.; Colina, C. M.; Figg, C. A.; Kaar, J. L.; Matyjaszewski, K.; Simakova, A.; Sumerlin, B. S., Next generation protein-polymer conjugates. *AIChE J.* **2018,** *64* (9), 3230-3245.
44. Qi, Y. Z.; Simakova, A.; Ganson, N. J.; Li, X. H.; Luginbuhl, K. M.; Ozer, I.; Liu, W. G.; Hershfield, M. S.; Matyjaszewski, K.; Chilkoti, A., A brush-polymer/exendin-4 conjugate reduces blood glucose levels for up to five days and eliminates poly(ethylene glycol) antigenicity. *Nat. Biomed. Eng.* **2017,** *1* (1), 0002.
45. Isarov, S. A.; Pokorski, J. K., Protein ROMP: Aqueous Graft-from Ring-Opening Metathesis Polymerization. *ACS Macro Lett.* **2015,** *4* (9), 969-973.
46. Lu, J.; Wang, H.; Tian, Z.; Hou, Y.; Lu, H., Cryopolymerization of 1,2-Dithiolanes for the Facile and Reversible Grafting-from Synthesis of Protein–Polydisulfide Conjugates. *J. Am. Chem. Soc.* **2020,** *142* (3), 1217-1221.
47. Wang, H.; Hu, Y.; Wang, Y.; Lu, J.; Lu, H., Doxorubicin@ PEPylated interferon-polydisulfide: A multi-responsive nanoparticle for enhanced chemo–protein combination therapy. *Giant* **2021,** *5*, 100040.
48. Tsuyuki, H.; Van Kley, H.; Stahmann, M. A., The Preparation and Physical Properties of Polypeptidyl Proteins1,2. *J. Am. Chem. Soc.* **1956,** *78* (4), 764-767.
49. Sela, M.; Arnon, R., Studies on the Chemical Basis of the Antigenicity of Proteins .3. Role of Rigidity in the Antigenicity of Polypeptidyl Gelatins. *Biochem. J.* **1960,** *77*, 394-399.
50. Pelegri-O'Day, E. M.; Lin, E. W.; Maynard, H. D., Therapeutic protein-polymer conjugates: advancing beyond PEGylation. *J. Am. Chem. Soc.* **2014,** *136* (41), 14323-14332.
51. Chen, C.; Wah Ng, D. Y.; Weil, T., Polymer bioconjugates: Modern design concepts toward precision hybrid materials. *Prog. Polym. Sci.* **2020**, 101241.
52. Zhang, P.; Sun, F.; Liu, S. J.; Jiang, S. Y., Anti-PEG antibodies in the clinic: Current issues and beyond PEGylation. *J. Controlled Release* **2016,** *244*, 184-193.
53. Wurm, F.; Klos, J.; Rader, H. J.; Frey, H., Synthesis and Noncovalent Protein Conjugation of Linear-Hyperbranched PEG-Poly(glycerol) alpha,omega(n)-Telechelics. *J. Am. Chem. Soc.* **2009,** *131* (23), 7954-7955.
54. Hou, Y.; Lu, H., Protein PEPylation: A New Paradigm of Protein–Polymer Conjugation. *Bioconjugate Chem* **2019,** *30* (6), 1604-1616.

55. Hu, Y.; Wang, D.; Wang, H.; Zhao, R.; Wang, Y.; Shi, Y.; Zhu, J.; Xie, Y.; Song, Y.-Q.; Lu, H., An urchin-like helical polypeptide-asparaginase conjugate with mitigated immunogenicity. *Biomaterials* **2021,** *268*, 120606.